Front. Earth Sci. 2024, 18(4): 714−731
https://doi.org/10.1007/s11707-024-1104-3

RESEARCH ARTICLE

Geochemical characteristics and origin of crude oil and natural gas in different areas of Wenchang-A Sag, Pearl River Mouth Basin, South China Sea

Xiaoyan FU[1], Shijia CHEN (✉)[1], Jungang LU[1,2,3], Mingzhu LEI[2]

1 Exploration and Development Research Institute of PetroChina Southwest Oil and Gas Field, Chengdu 610051, China
2 School of Geoscience and Technology, Southwest Petroleum University, Chengdu 610500, China
3 Hainan Branch of China National Offshore Oil Corporation Ltd., Zhanjiang 524000, China

Abstract Complex hydrocarbon distributions characterize the Wenchang-A Sag. Systematic study of the geochemical characteristics of crude oil, natural gas and source rocks and their genetic relationship is still needs to be completed. The Rock-Eval, kerogen maceral, vitrinite reflectance, saturated hydrocarbon gas chromatography-mass spectrometry, natural gas components, carbon isotopes, and light hydrocarbon were performed. 1) Crude oil is classified based on four factors: wax content, the presence of C_{27} diasteranes, the regular steranes αα20RC_{27}-αα 20RC_{28}-αα20RC_{29}, and the bicadinanes characteristics. Class I crude oil has high wax and C_{27} diasteranes. For Class II crude oil, the regular steranes are in ‘L’- shaped distribution, and the content of bicadinanes is shallow. Class III crude oil has soft wax and C_{27} diasteranes, and regular steranes in the reverse ‘L’-shaped distribution, with a high peak degree of bicadinanes. For Class IV crude oil, regular steranes are in ‘V’-shaped distribution, with high peak bicadinane. 2) Class I crude oil comes from source rocks in area C. Class II crude oil comes from source rocks in areas D and E. Class III crude oil comes from areas A, and B. Class IV crude oil comes from source rocks in area A. 3) The source of natural gas in Group I is hydro propylene, and natural gas in Group II is humic. Natural gas in Group III is mixed. Groups I and II are kerogen cracking gas, and group III is a mixture of crude oil secondary cracking gas and kerogen cracking gas. Natural gas in Groups I and II mainly come from local source rocks, and Group III has mixed source characteristics. In the future, oil exploration can continue in Areas C and D, and more favorable areas for gas exploration are Areas C, D, and E.

Received February 19, 2023; accepted September 21, 2023

E-mail: csj199131010015@163.com

Keywords organic geochemistry, origin, geochemical characteristics, crude oil, natural gas

1 Introduction

The Wenchang-A Sag, located in the Zhu III Depression of the Pearl River Mouth Basin (PRMB) (Fig. 1(a)), is a Cenozoic extensional graben basin at the continental margin (Jiang et al., 2009; Jiang et al., 2021). Since hydrocarbon exploration began in the 1980s (Wu, 1984; Huang et al., 2003), a series of oil and gas fields have been discovered in the Wenchang-A Sag, which is grouped into five areas, namely Areas A, B, C, D, and E (Fig. 1(b)). Area A lies in the western part of the sag and is mainly found with oil reservoirs, while Area E, located in the eastern sag, develops gas reservoirs. Moreover, Areas B, C, and D are dominated by gas reservoirs, yet have locally-developed reservoirs (Fig. 1(b)). This research, based on actual production data, investigates the geochemical characteristics of the source rock and hydrocarbons and considers that the primary source rock for the study area in only the Oligocene Enping Formation source rock (Jiang et al., 2009; Quan et al., 2015).

Previous studies indicate that the source rock of the Wenchang-A Sag is humic and has reached the mature stage (Fu et al., 2011; Quan et al., 2015). There are differences in oil and gas distribution in the study area. Areas A and B are dominated by oil reservoirs, and areas C, D, and E are dominated by gas reservoirs (Fig. 1(b)). Further analysis is needed to understand the reasons for the varied distribution of oil and gas throughout the region, as well as the geochemical properties and origins of these hydrocarbons. Hence, this study first investigates the characteristics of the source rock and then thoroughly reviews the source rocks of the Wenchang-A Sag using

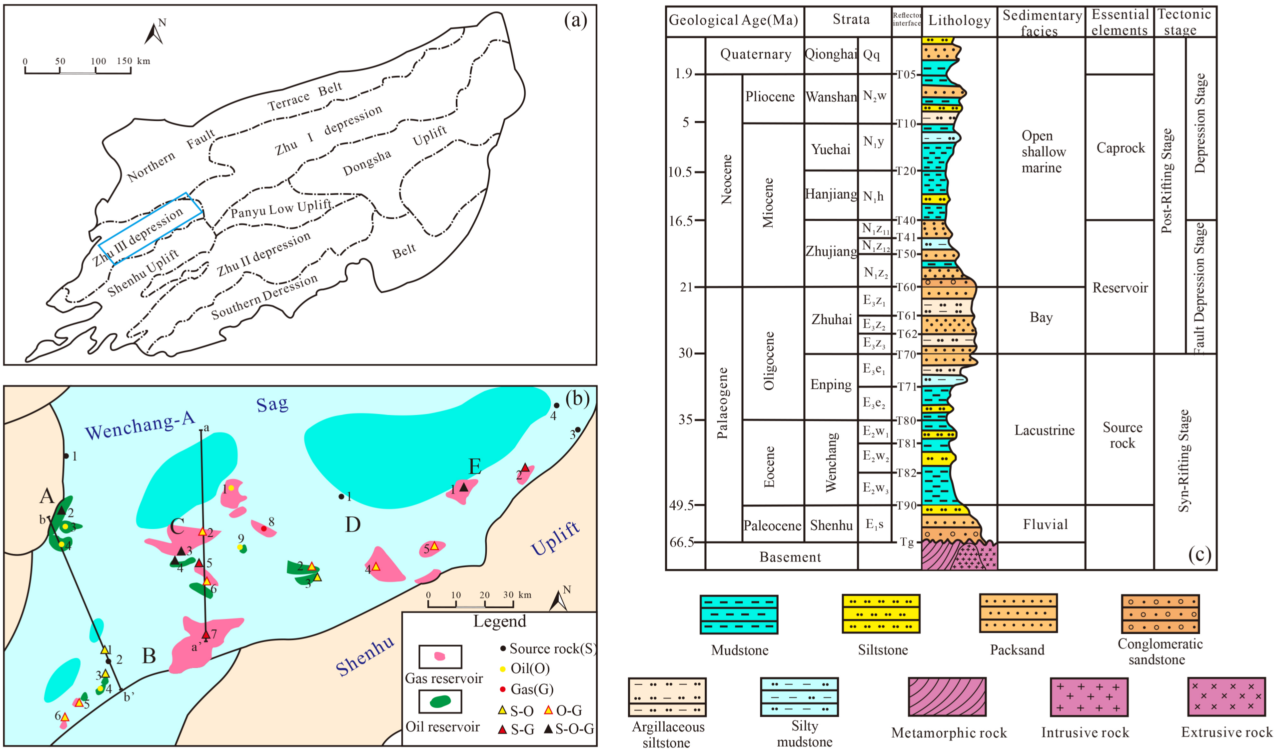

Fig. 1 (a) PRMB geographic location map. (b) Distribution of oil and gas reservoirs and sampling wells in Wenchang-A Sag (modified on the basis of information provided by Zhanjiang Branch of China National Offshore Oil Corporation). (c) Schematic stratigraphic column in Zhu III Depression of PRMB (modified from Cheng et al., 2015; Quan, 2018).

multiple geochemical approaches, such as Rock-Eval pyrolysis, kerogen maceral analysis, and vitrinite reflectance measurement. Furthermore, the geochemical characteristics and source of crude oil are identified by mass spectrometry-gas chromatography of total, light and saturated hydrocarbons. Meanwhile, the origin of natural gas is determined by gas composition, carbon isotope ratio, and light hydrocarbons. The results of this study are expected to clarify the geochemical characteristics and origin of oil and gas in the study area, and identify the main control factors contributing to the differentiated planar distribution of oil and gas reservoirs, and thus to provide the theoretical guidance for the deployment of hydrocarbon exploration in the Wenchang-A Sag.

2 Geological setting

PRMB is in the northern South China Sea, covering an area of about 175000 m^2 and mainly featuring Cenozoic deposits (Wu, 1984; Jiang et al., 2009; Quan, 2018), and contains eight structural units. Namely Zhu I, II, and III Depressions, Shenhu Uplift, Panyu Low Uplift, Dongshan Uplift, Southern Depression, and Northern Fault Belt. The Wenchang-A Sag is located in the northern Zhu III Depression (Fig. 1(a)). The Wenchang-A Sag is characterized by faulting in the south, overlapping in the north, and transition in the center. Due to the fault belt and local low relief, many sub-sags develop sequentially inside this sag, named A−E (Fig. 1(b)).

Since the Cenozoic, PRMB has undergone three tectonic evolution stages, namely rift, fault depression, and depression stages (Xu and Huang, 2000; Xiao et al., 2009). From bottom to top, it mainly develops the Palaeogene Wenchang, Enping, and Zhuhai Formations, as well as the Neogene Zhujiang, Hanjiang, and Yuehai Formations (Fig. 1(c)). The second member of the Enping Formation is encountered in the Wenchang-A Sag, and the Enping Formation is found with thick source rocks (Figs. 2(a) and 2(b)). During the fault depression stage of the late Oligocene (30−16.5 Ma), the Zhuhai and Zhujiang Formations are deposited, which serve as the main reservoir rocks for the Zhu III Depression (Cheng et al., 2015; Quan et al., 2015), and the second member of the Zhuhai Formation has the most considerable thickness (Figs. 2(a) and 2(b)). PRMB has entered the depression stage since 16.5 Ma, which is associated with weakening tectonic movement and sedimentation of finer mudstone and siltstone that evolve into the regional cap rock of the Zhu III Depression (Chen et al., 2020). Due to tectonic movement, Area C of the central Wenchang-A Sag is seen with the highest development of faults; and the seismic profile from the sag center in Area C to the sag margin presents closely spaced faults (Fig. 2(a)). As for Areas A and B in the sag margin, they show fewer faults in the seismic profile (Fig. 2(b)).

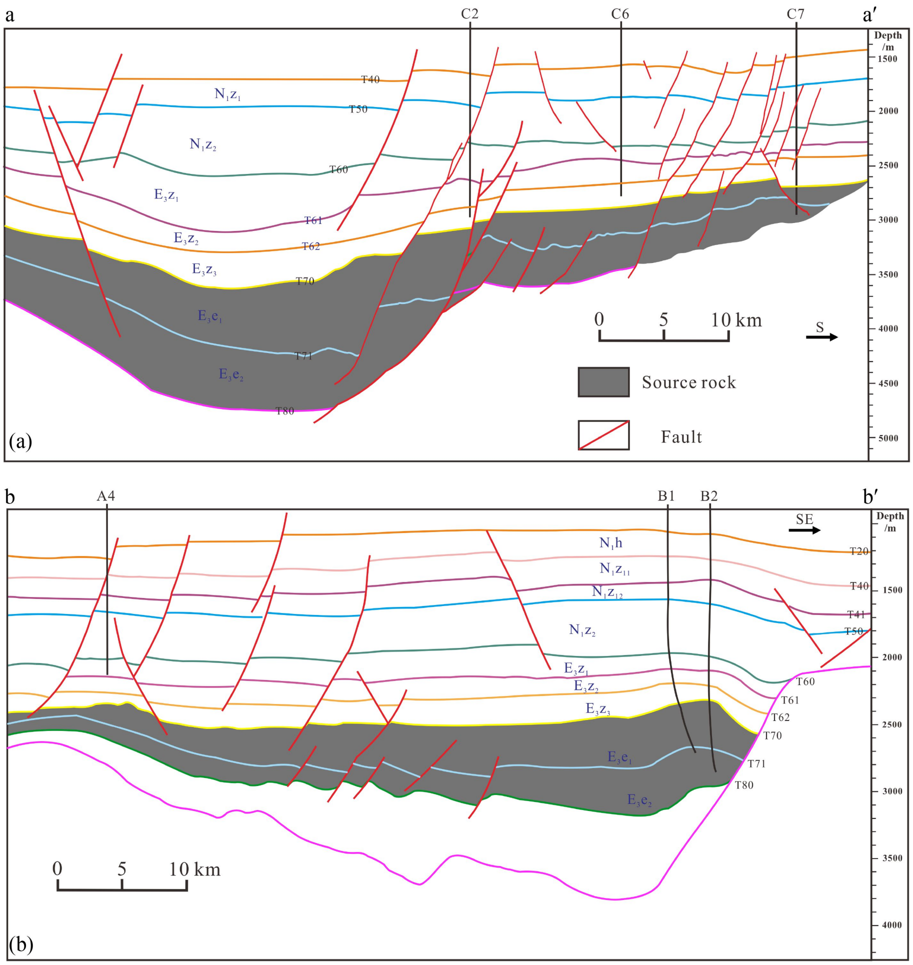

Fig. 2 Schematic sections along lines a–a' and b–b' in Fig. 1(b).

3 Materials and methodology

3.1 Materials

A total of 109 mudstone samples were collected from 15 wells. Rock-Eval pyrolysis used 68 samples. A total of 17 vitrinite reflectances were measured. The data are shown in Table 1. Saturated hydrocarbon gas chromatography-mass spectrometry (GC-MS) used 24 mudstone samples. Crude oil samples were collected from 19 wells. Data on the physical properties and components of crude oil are provided by CNOOC Zhanjiang Branch (Table 2). GC-MS of 26 crude oils was determined. Specific sample information is shown in Table 3. Natural gas samples come from 15 wells. The types and distribution of sampling wells are shown in Fig. 1(b).

3.2 Methods

1) Rock pyrolysis

Samples are pre-treated by stepwise acid washing to remove unwanted substances, such as carbonate and silicate, and dried using filter paper. The source rock samples are crushed and ground into 0.07–0.15 mm, and the test instrument is the Rock-Eval 6 apparatus. The flow rate of high-purity nitrogen gas is 50 mL/min; that of hydrogen, 30 mL/min; and that of air, 300 mL/min. The initial temperature is 300°C and held for 3 min, and then the temperature is raised at a rate of 25°C/min to 650°C.

2) Determination of kerogen maceral

Kerogen needs to be extracted first. The mudstone samples with TOC ⩾ 0.4% are selected (25/20-mesh; 50 g of each sample) and mixed with HCl, NaOH, and heavy liquid, successively. Then, they are separated by ultrasonically assisted centrifugal separation to extract the kerogen in the upper part. Afterwards, the kerogen is extracted and transformed into thin sections by utilizing the glycerol method of thin section preparation. Finally, thin sections of kerogen prepared were observed using the LEICA DM400B biological microscope, and maceral characteristics were summarized. These tests are carried out in the laboratory of CNOOC Zhanjiang Branch Co. Ltd.

3) Vitrinite reflectance

The vitrinite reflectance refers to the percentage of the reflection light intensity from the polished vitrinite

Table 1 Statistical table of *Ro* in Wenchang-A Sag

Well name	Depth/m	Formation	Lithology	Sample type	R_o/%
B2	3170	E_3e_1	Mudstone	Rock debris	0.79
B2	3215	E_3e_1	Mudstone	Rock debris	0.78
B2	3235	E_3e_1	Mudstone	Rock debris	0.70
B2	3285	E_3e_1	Mudstone	Rock debris	0.70
C3	4257	E_3e_1	Mudstone	Rock debris	1.08
C4	4228	E_3e_1	Mudstone	Rock debris	1.01
C7	3640	E_3e_1	Mudstone	Rock debris	0.87
C7	3956	E_3e_1	Mudstone	Rock debris	1.10
D1	5020	E_3e_1	Mudstone	Rock debris	1.29
D1	5050	E_3e_1	Mudstone	Rock debris	1.24
E1	4712	E_3e_1	Mudstone	Rock debris	1.22
E1	4746	E_3e_1	Mudstone	Rock debris	1.18
E3	3967	E_3e_1	Mudstone	Rock debris	0.98
E3	4020	E_3e_1	Mudstone	Rock debris	1.02
E3	4113	E_3e_1	Mudstone	Rock debris	1.07
E3	4135	E_3e1	Mudstone	Rock debris	1.07

surface to the normal incidence light with the wavelength of 546 nm ± 5 nm (green light) (Hunt, 1979). The adopted instrument is the MPV-COMPACT microscope photometer, which is manufactured by Leitz (Germany). The tests of vitrinite reflectance of the source rock are performed with a temperature of 23°C ± 3°C and relative humidity below 70%.

4) Gas chromatography-mass spectrometry (GC-MS) of saturated hydrocarbons

Soxhlet extraction method, using chloroform as solvent, is used to extract soluble organic matter bitumen from the sample. After bitumen is removed by *n*-hexane, saturated hydrocarbons, aromatic hydrocarbons, and non-hydrocarbons are separated by silica gel-alumina (3:2) chromatography. The HP5890-5972 GC-MS analyzer is used to analyze the saturated hydrocarbon fractions, equipped with a 60.00 m × 0.32 mm × 0.25 μm capillary column. The starting temperature of heating is 100°C; the carrier gas is helium; the constant flow mode is adopted; the ion source temperature is 230°C; and the inlet temperature is set to 310°C.

5) Natural gas composition

After depressurization, drying, and filtration, the sample is tested using HP 5890 II 600501 GC system. The gas output pressure is set at 80 psi, and the test is performed. The carrier gas is helium. We start at temperature of 40°C and held for 10 min; then, it is heated at 5°C/min to 180°C and held for 10 min.

6) Natural gas carbon isotope ratios

The test is performed, using the IsoPrime 100 gas source stable isotope ratio spectrometer and Agilent 7890A gas chromatograph (Instrument No. D01JS016). The initial temperature of the GC system is 35°C. The temperature is subsequently elevated at a rate of 8°C/min to 80°C, and finally stimulated at a rate of 5°C/min to 260°C and held for 10 min (Li et al., 2019; Lu, 2021).

7) Light natural gas hydrocarbons

The analysis of light hydrocarbons of natural gas is performed using the HP Agilent 6890N GC system, equipped with the HP PONA, 50 m × 0.2 mm × 0.5 mm chromatographic column, and flame ionization detector (FID). The temperature is initially set below 30°C and held for about 15 min. Then, it is heated to 70°C at 15°C/min and kept for 2 min. Furthermore, it is raised to 150°C at 3°C/min and held for 10 min. At last, the temperature is elevated to 270°C at 5°C/min.

4 Results

4.1 Geochemical characteristics of source rocks

4.1.1 Organic matter types

Organic matter types determine kerogen's ability to produce oil or gas. The organic matter that is more of the sapropel type tends to have oil in the mature stage, while the humic organic matter generates a massive volume of natural gas during the mature stage (Huang et al., 1984; Chen et al., 2021; Li and Gong, 2022). Overall, humic organic matter is distributed on the edge of the sag, while sapropelic organic matter is distributed in the middle of the sag. The source rocks of the gas reservoir are mainly humic organic matter, and the reservoirs are distributed in the sapropelic organic matter area. Areas A and B also have local sapropelic source rocks (Fig. 3).

Table 2 Physical properties and composition of crude oil

Type	Well	Depth/m	Formation	Sample	Density /(g·cm^{-3})	Wax/%	Sulfur/%	Saturate/%	Aromatic/%	Nonhydrocarbon/%	Asphaltenes/%
Class I	A3	1692.5	N_1z	Oil	0.79	4.51	0.05	87.56	9.42	2.02	1.01
	A3	1694	N_1z	Oil	0.78	5.20	0.06	80.00	14.89	4.66	0.46
	A3	1699.5	N_1z	Oil	0.78	4.10	0.05	80.36	13.24	3.66	2.74
	A3	1700	N_1z	Oil	0.78	4.16	0.06	81.82	13.13	3.36	1.68
	A3	1707.5	N_1z	Oil	0.78	3.34	0.05	78.99	14.37	3.32	3.32
	A4	2257	N_1z	Oil	0.78	3.24	0.05	65.00	12.00	21.00	2.00
	B4	1791	N_1z	Oil	0.76	2.21	0.05	–	–	–	–
	B4	2240	E_3z	Oil	0.78	4.99	0.07	86.67	10.25	3.08	0.00
	B4	2308	E_3z	Oil	0.75	0.34	0.06	92.44	5.04	2.52	0.00
	B4	2365	E_3z	Oil	0.76	0.91	0.06	82.58	7.29	10.13	0.00
	B4	2417	E_3z	Oil	0.75	1.42	0.06	90.24	7.45	2.31	0.00
Class II	C1	3129.4	N_1z	Oil	0.79	6.53	0.02	69.00	9.00	21.00	1.00
	C1	3153.7	N_1z	Oil	0.76	3.24	0.02	72.00	9.00	18.00	1.00
	C1	3153.7	N_1z	Oil	0.76	3.56	0.02	81.00	6.00	12.00	1.00
	C1	3176	N_1z	Oil	0.77	3.38	0.02	68.00	9.00	21.00	2.00
	C1	3352	E_3z	Oil	0.76	4.28	0.02	87.00	8.00	4.00	1.00
	C1	3699	E_3z	Oil	0.76	3.58	0.02	89.00	9.00	1.00	1.00
	C1	3799	E_3z	Oil	0.77	3.95	0.01	85.00	10.00	4.00	1.00
	C1	4000	E_3z	Oil	0.76	3.24	0.02	82.00	11.00	5.00	2.00
	C4	3543	E_3z	Oil	0.83	–	–	89.61	7.27	2.73	0.40
	C4	3588.2	E_3z	Oil	0.82	–	–	86.47	7.49	4.39	1.65
	C4	3638	E_3z	Oil	0.80	–	–	88.18	7.42	3.17	1.23
	E1	3695	E_3z	Oil	0.78	2.38	0.02	85.51	10.14	3.26	1.08
	E1	3710	E_3z	Oil	0.77	2.73	0.01	–	–	–	–
	D2	3971	E_3z	Oil	0.80	7.91	0.03	82.15	11.90	4.25	1.70
	D2	3975	E_3z	Oil	0.78	2.74	0.02	87.41	9.35	2.52	0.72
	D3	2539	N_1z	Oil	0.82	3.70	0.01	91.73	6.48	1.52	0.27
	D5	3415	E_3z	Oil	0.76	3.36	0.03	–	–	–	–
	D5	3543	E_3z	Oil	0.75	3.56	0.02	–	–	–	–
Class III	A2	2350	N_1z	Oil	0.75	0.47	0.03	81.15	9.95	6.28	2.62
	C2	3903.3	E_3z	Oil	0.76	0.87	0.03	85.97	11.86	1.08	1.08
Class IV	B3	2904	E_3z	Oil	0.76	0.41	0.02	75.94	11.13	11.46	1.47
	B5	2968	E_3z	Oil	0.81	0.38	0.01	81.68	13.35	4.32	0.65

The types of organic matter in the study area vary in different sub-sags (Fig. 4). Organic matter types of formation intervals vary at different depths. For example, in wells B2 and D1, sapropelic and humic organic matter occur vertically alternately. Planar and vertical variations in organic matter types may contribute to the differentiated hydrocarbon distribution across the study area.

4.1.2 Hydrocarbon generation potential of source rocks

Total organic carbon (TOC) is the amount of organic carbon in a rock per unit mass (Lu et al., 2021; Tang et al., 2022). It also includes carbon in soluble organic matter, and is often used to represent organic matter abundance (Dehyadegari, 2021; Su et al., 2021; Huang et al., 2022). S_2 illustrates the content of the pyrolysis hydrocarbon of kerogen at 300°C–500°C, and hence, it can be used as a measure of the hydrocarbon generation potential of source rocks (Peters and Cassa, 1994). The quality in Areas A and B is poor and fair, and the quality of source rocks in Areas C and D is better. There is a diverse range of source rock quality across various wells in the E area. E2 is the best, followed by E1, and E3 is the

Table 3 Molecular geochemical data of source rocks and crude in Wenchang-A Sag

Type	Well	Depth /m	Formation	Sample	TIC			m/z 217					m/z 412	m/z 191		
					1	2	3	4	5	6	7	8	9	10	11	12
Class I	A3	1670	N_1z_1	Oil	3.13	0.43	0.15	0.81	1.11	0.42	0.45	0.11	1.11	0.69	0.59	0.07
	A3	1692.5	N_1z_1	Oil	2.74	0.46	0.16	0.77	1.12	0.41	0.45	0.13	1.00	0.69	0.58	0.07
	A3	1699.5	N_1z_1	Oil	2.75	0.46	0.18	0.72	1.02	0.47	0.49	0.12	1.18	0.68	0.59	0.08
	A3	1700	N_1z_1	Oil	2.67	0.44	0.16	0.81	1.13	0.46	0.51	0.13	1.21	0.71	0.59	0.07
	A3	1707.5	N_1z_1	Oil	2.96	0.57	0.22	0.80	1.07	0.39	0.49	0.16	1.04	0.68	0.58	0.08
	A4	2257	N_1z_2	Oil	3.36	0.44	0.39	0.63	1.11	0.30	0.55	0.21	1.19	0.71	0.72	0.08
	A4	2321	N_1z_2	Oil	3.35	0.43	0.34	0.62	1.04	0.35	0.54	0.20	1.17	0.72	0.71	0.05
	B4	2230	E_3z_1	Oil	1.58	2.21	0.72	0.84	1.08	0.39	0.38	0.15	1.78	0.45	0.40	0.16
	B6	2904	E_3z_1	Oil	2.92	0.59	0.21	0.61	1.18	0.38	0.41	0.24	1.52	0.58	0.57	0.07
	C6	3229.59	N_1z	Oil	3.27	0.30	0.13	0.64	1.28	0.42	0.49	0.02	1.62	0.64	0.78	0.08
Class II	C1	3665	N_1z_2	Oil	1.33	0.36	0.25	0.69	0.44	0.38	0.39	0.12	0.28	0.59	0.34	0.13
	C1	3700	E_3z	Oil	1.81	0.52	0.24	0.68	0.42	0.39	0.36	0.11	0.27	0.61	0.32	0.21
	C4	3543	E_3z_3	Oil	2.08	0.35	0.15	0.82	0.83	0.45	0.50	0.49	0.66	0.80	0.92	0.15
	C4	3588.2	E_3z_3	Oil	2.18	0.34	0.12	0.89	0.82	0.48	0.54	0.50	0.55	0.81	0.89	0.13
	C4	3638	E_3z_3	Oil	2.50	0.34	0.16	1.03	0.81	0.46	0.54	0.53	0.54	0.82	0.88	0.29
	D4	2871.5	E_3z_1	Oil	2.35	0.74	0.31	1.15	0.61	0.42	0.46	0.26	0.06	0.53	0.34	0.09
	D4	3343.9	E_3z_2	Oil	1.90	0.83	0.42	0.91	0.65	0.43	0.46	0.23	0.46	0.56	0.38	0.12
	D4	3683.45	E_3z_2	Oil	1.84	0.75	0.37	0.79	0.53	0.50	0.43	0.21	0.42	0.49	0.40	0.14
	E1	4210	E_3z_3	Oil	2.92	0.51	0.17	1.34	0.65	0.50	0.49	0.60	0.53	0.51	0.39	0.07
	E1	4305	E_3e_1	Oil	2.63	0.52	0.15	1.06	0.72	0.48	0.53	0.51	0.46	0.51	0.35	0.08
	E1	4494	E_3e_1	Oil	1.94	0.54	0.12	1.20	0.62	0.42	0.53	0.74	0.31	0.53	0.39	0.10
Class III	B1	2670.6	E_3z_1	Oil	3.57	0.72	0.19	0.74	0.42	0.39	0.43	0.26	1.58	0.57	0.35	0.06
	C9	3351	N_1z	Oil	1.33	1.21	0.90	0.67	0.56	0.38	0.40	0.15	1.59	0.48	0.32	0.14
Class IV	A2	2350	N_1z_2	Oil	3.24	0.59	0.18	0.65	0.24	0.35	0.42	0.12	1.42	0.32	0.26	0.09
	A2	2384	N_1z_2	Oil	2.00	0.80	0.42	0.64	0.23	0.37	0.41	0.09	1.43	0.45	0.31	0.07
	C2	3375	N_1z	Oil	1.45	1.06	0.49	0.84	0.25	0.34	0.45	0.20	1.58	0.78	0.78	0.12
Area A	A1	3310	E_3e_2	Mudstone	1.61	0.85	0.46	0.81	0.52	0.48	0.48	0.18	0.90	0.51	0.31	0.32
	A1	3340	E_3e_2	Mudstone	1.59	0.81	0.43	0.72	0.53	0.47	0.42	0.21	0.95	0.43	0.41	0.31
	A1	3350	E_3e_2	Mudstone	1.58	0.48	0.35	0.89	0.57	0.48	0.45	0.19	0.93	0.46	0.42	0.32
	A1	3362	E_3e_2	Mudstone	1.62	0.83	0.42	0.67	0.57	0.42	0.41	0.25	0.94	0.48	0.40	0.29
	A1	3425	E_3e_2	Mudstone	1.28	0.54	0.33	0.78	0.54	0.49	0.47	0.24	0.96	0.50	0.44	0.35
	A2	3402	E_3e_1	Mudstone	2.34	0.57	0.28	0.62	0.22	0.43	0.39	0.14	1.24	0.43	0.28	0.21
	A2	3425	E_3e_1	Mudstone	3.71	1.63	0.30	0.67	0.23	0.44	0.39	0.08	1.11	0.43	0.30	0.12
Area B	B1	4124	E_3e_1	Mudstone	1.87	1.28	0.79	0.48	0.41	0.39	0.38	0.11	1.19	0.60	0.30	0.15
Area C	C7	3648	E_3e_1	Mudstone	3.20	0.48	0.19	0.93	0.87	0.47	0.55	0.07	1.81	0.72	0.84	0.05
	C7	3666	E_3e_1	Mudstone	3.90	1.26	0.34	0.57	0.89	0.46	0.52	0.08	2.48	0.61	0.91	0.08
	C7	3696	E_3e_1	Mudstone	3.07	1.46	0.51	0.59	0.91	0.44	0.51	0.07	1.65	0.62	0.98	0.14
	C7	3722	E_3e_1	Mudstone	4.34	1.01	0.25	0.62	0.87	0.42	0.52	0.09	1.23	0.66	0.95	0.06
	C7	3740	E_3e_1	Mudstone	3.34	0.85	0.22	0.57	0.86	0.45	0.53	0.10	2.34	0.57	0.76	0.10
	C7	3780	E_3e_1	Mudstone	2.70	0.82	0.27	0.71	0.92	0.45	0.51	0.12	1.12	0.69	0.96	0.19
	C7	3820	E_3e_1	Mudstone	4.31	0.87	0.22	0.71	0.88	0.45	0.52	0.19	1.42	0.97	0.73	0.05

(*continued*)

Type	Well	Depth /m	Formation	Sample	TIC			m/z 217					m/z 412	m/z 191		
					1	2	3	4	5	6	7	8	9	10	11	12
Area D	D1	4507.55	E_3e_1	Mudstone	1.12	0.70	0.45	1.03	0.57	0.43	0.41	0.30	0.29	0.56	0.38	0.31
	D1	4512.15	E_3e_1	Mudstone	1.08	0.71	0.44	1.06	0.58	0.43	0.39	0.32	0.32	0.57	0.39	0.31
	D3	3673	E_3e_1	Mudstone	3.14	0.84	0.77	0.62	0.74	0.39	0.42	0.09	0.20	0.92	0.32	0.14
Area E	E1	4348	E_3e_1	Mudstone	3.19	0.62	0.19	1.22	0.68	0.45	0.44	0.23	0.40	0.51	0.30	0.12
	E1	4380	E_3e_1	Mudstone	1.81	0.30	0.16	1.36	0.54	0.44	0.44	0.21	0.34	0.50	0.28	0.31
	E1	4454	E_3e_1	Mudstone	3.05	0.30	0.19	1.03	0.61	0.46	0.43	0.22	0.35	0.56	0.37	0.10
	E1	4514	E_3e_1	Mudstone	1.61	0.30	0.18	1.02	0.83	0.46	0.44	0.34	0.24	0.49	0.36	0.25
	E1	4522	E_3e_1	Mudstone	2.05	0.20	0.11	1.11	0.86	0.45	0.43	0.22	0.38	0.49	0.30	0.21
	E1	4542	E_3e_1	Mudstone	1.51	0.34	0.22	1.08	0.78	0.46	0.44	0.22	0.44	0.53	0.39	0.30

Notes: 1 = Pr/Ph (Pristine/ Phytane); 2 = Pr/nC_{17}; 3 = Ph/nC_{18}; 4 = $\sum C_{27}$RSt /$\sum C_{29}$RSt (RSt: regular sterane); 5 = $\sum C_{27}$diasterane/$\sum C_{27}$RSt; 6 = $C_{29}\alpha\beta\beta/(\alpha\beta\beta + \alpha\alpha\alpha)$; 7 = $C_{29}\alpha\alpha\alpha$20S/ (20S + 20R); 8 = $\sum C_{30}$-4MSt/C_{29} RSt (MSt: methyl sterane); 9 = bicadinanes/C_{30}hopane((W+T)/C_{30}H); 10 = Ts/(Ts+Tm) (Ts: 18α(H)-C_{27} trisnorhopane, Tm: 17α(H)-C_{27} trisnorhopane); 11 = C_{29}Ts/C_{29}Hopane; 12 = G/C_{30}H (G: gammacerane).

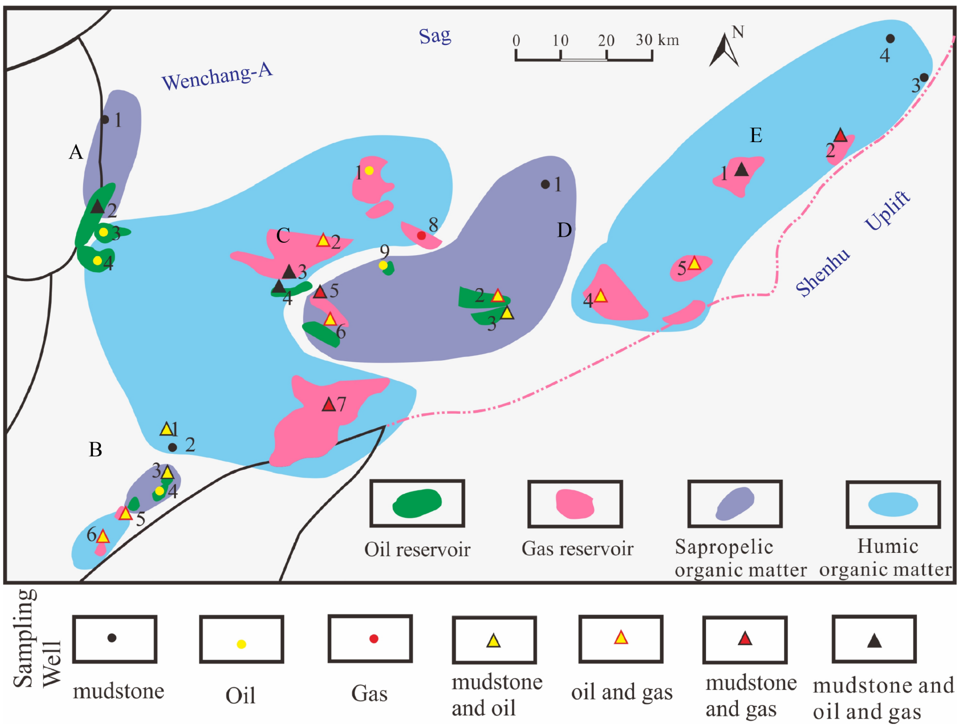

Fig. 3 Plane distribution of organic matter types in Wenchang-A Sag.

worst (Fig. 5). It shows that source rocks in Area E also have the potential to generate oil and gas.

Vitrinite reflectance (R_o) is an essential measure of source rock maturity (Wu and Gu, 1986). R_o of the source rock in the study area is 0.70%–1.29% (Table 1), averaging 1.01%. This indicates that the source rock throughout the sag has entered the mature stage. The maturity of source rocks gradually increased from the south-west to the north-east of the study area, i.e., from Areas B to E.

4.2 Physical and compositional characteristics of crude oil

Crude oil is divided into four types according to its characteristics of physical properties, components and saturated hydrocarbon biomarker parameters. The characteristics and sources of different oils are analyzed below.

The crude oil of the Wenchang-A Sag is light oil, with a density of 0.75–0.83 g/cm^3 and averaging 0.78 g/cm^3 (Table 2). The wax content of crude oil varies greatly. Class I and II crude oils have a higher wax content, and

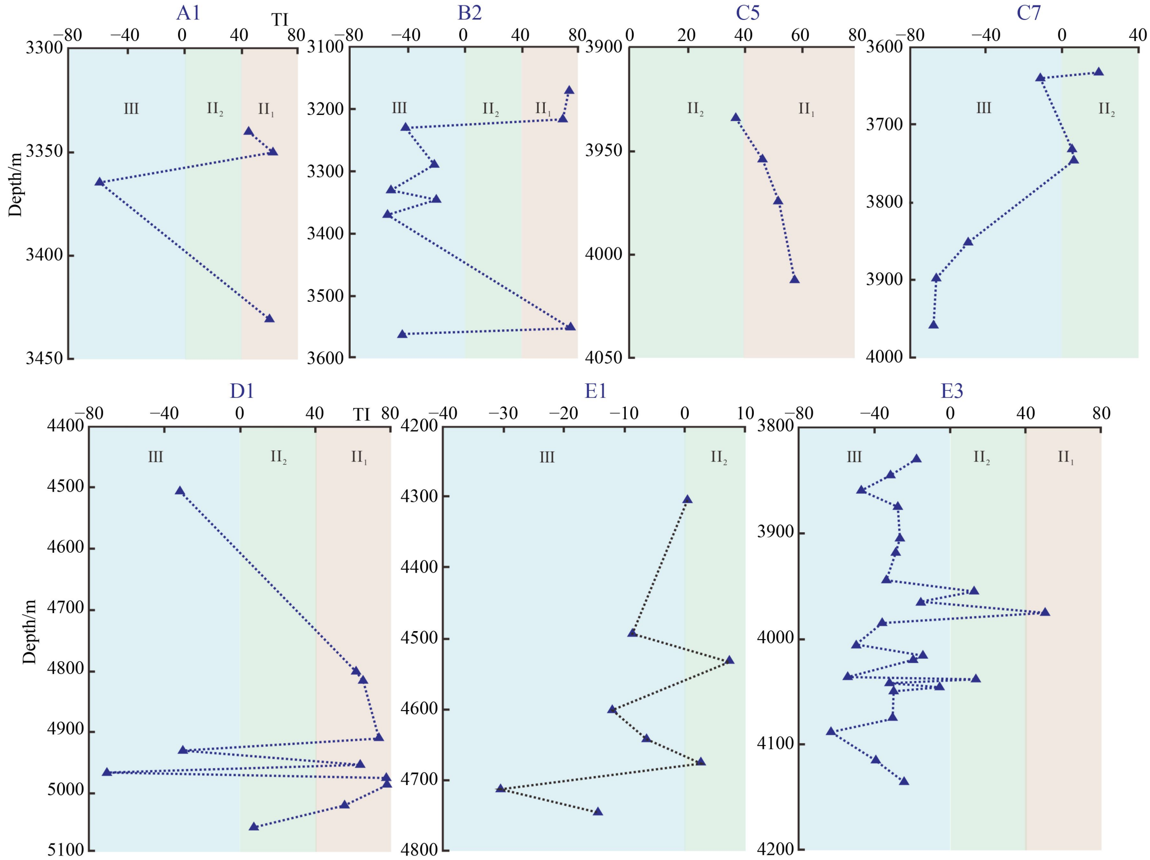

Fig. 4 Vertical variation characteristics of organic matter types in seven wells of Wenchang-A Sag.

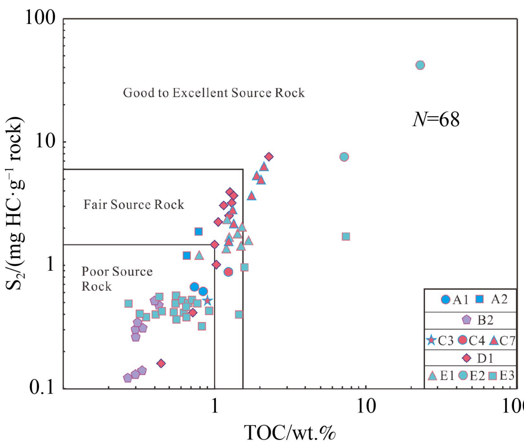

Fig. 5 Scatter plots of TOC and S_2 from Enping Formation source rocks in Wenchang-A Sag (Quan et al., 2015).

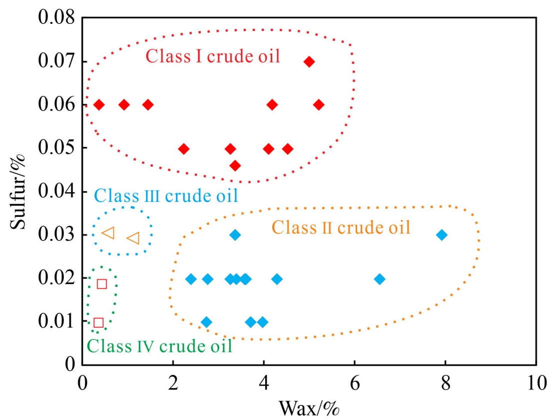

Fig. 6 Graph of intersection of sulfur and wax content in crude oil.

Class III and IV crude oils have a lower wax content (Fig. 6). Such differentiation may be related to the thermal maturation of source rocks. The sulfur content of crude oil in the study area is low. The content of saturated hydrocarbons is 65.00%–92.44%, and no notable content variation is seen among aromatic hydrocarbons, non-hydrocarbons, and asphaltenes (Table 2).

4.3 Biomarkers of source rocks and crude oil

The compounds pristane (Pr) and phytane (Ph) found in sediments are generated from the phytol side chain of chlorophyll. Pristane is formed in an environment containing oxygen, while phytane is produced through hydrogenation reduction. Accordingly, they indicate organic matter's sedimentary environment (Wood and Hazra, 2017). Pr/Ph below 1 stands for a reducing environment; 1–3, an oxidizing-reducing environment; above 3, an oxidizing environment (Hunt, 1979). The Pr/Ph values of the four types of crude oil in the study area and the source rocks of Enping Formation in different blocks are all greater than 1, indicating that they are all in a partial oxidizing environment. The *n*-alkanes of Class I and II crude oils are forward-type, while the *n*-alkanes of Class III and IV crude oils are completely peak-type (Fig. 7) (Table 3). The hopane characteristics of crude oil and source rocks in Wenchang A sag are similar, with C_{30} hopane as the main peak, 18α(H)-C_{29} trisnorhopane (C_{29}Ts) having a certain peak, and the content of gamma-cerane being low.

The difference between different types of crude oil is mainly reflected in the chromatogram of sterane and bicadinanes. C_{27}–C_{29} regular steranes (RSt) are derived from the steroids of eucaryon and algae (Tissot and Welte, 1984). 4-methyl steranes (MSt) is a frequent component in the Cenozoic lacustrine sediments in China (Huang et al., 1994). Bicadinanes (W + T) originate from resin compounds from higher plants and are formed in a more oxidizing sedimentary environment (Wood and Hazra, 2017; Milkov, 2018).

Class I crude oil in the study area has a high C_{27} diasteranes content. The distribution of *ααα*20RC_{27}-*ααα*20RC_{28}-*ααα*20RC_{29} is V-shaped, and the content of biscadinanes T is high. The bicadinanes / C_{30}hopane ((W + T) / C_{30}H) value is between 1.00 and 6.03 (Table 3), which is similar to the characteristics of source rocks in C area (Fig. 7). This kind of crude oil is mainly distributed in Areas A and B.

Class II crude oil also has a high diasteranes content. The distribution of *ααα*20RC_{27}-*ααα*20RC_{28}-*ααα*20RC_{29} in regular steranes is ‘L’-shaped distribution, and the bicadinanes content is shallow. The (W + T)/C_{30}H value is between 0.06 and 0.66 (Table 3), which is similar to the characteristics of source rocks in Area E (Fig. 7). This type of crude oil is mainly distributed in the Area C. Still, the crude oil of Wells D4 and E1 also have the same characteristics.

The diasteranes content in class III crude oil is low. The regular steranes of *ααα*20RC_{27}-*ααα*20RC_{28}-*ααα*20RC_{29} are distributed in the reverse ‘L’-shaped distribution. It has the high C_{29} regular steranes and bicadinanes content. The (W + T)/C_{30}H value is between 1.59 and 2.11, similar to the source rocks in Area B. The class III crude

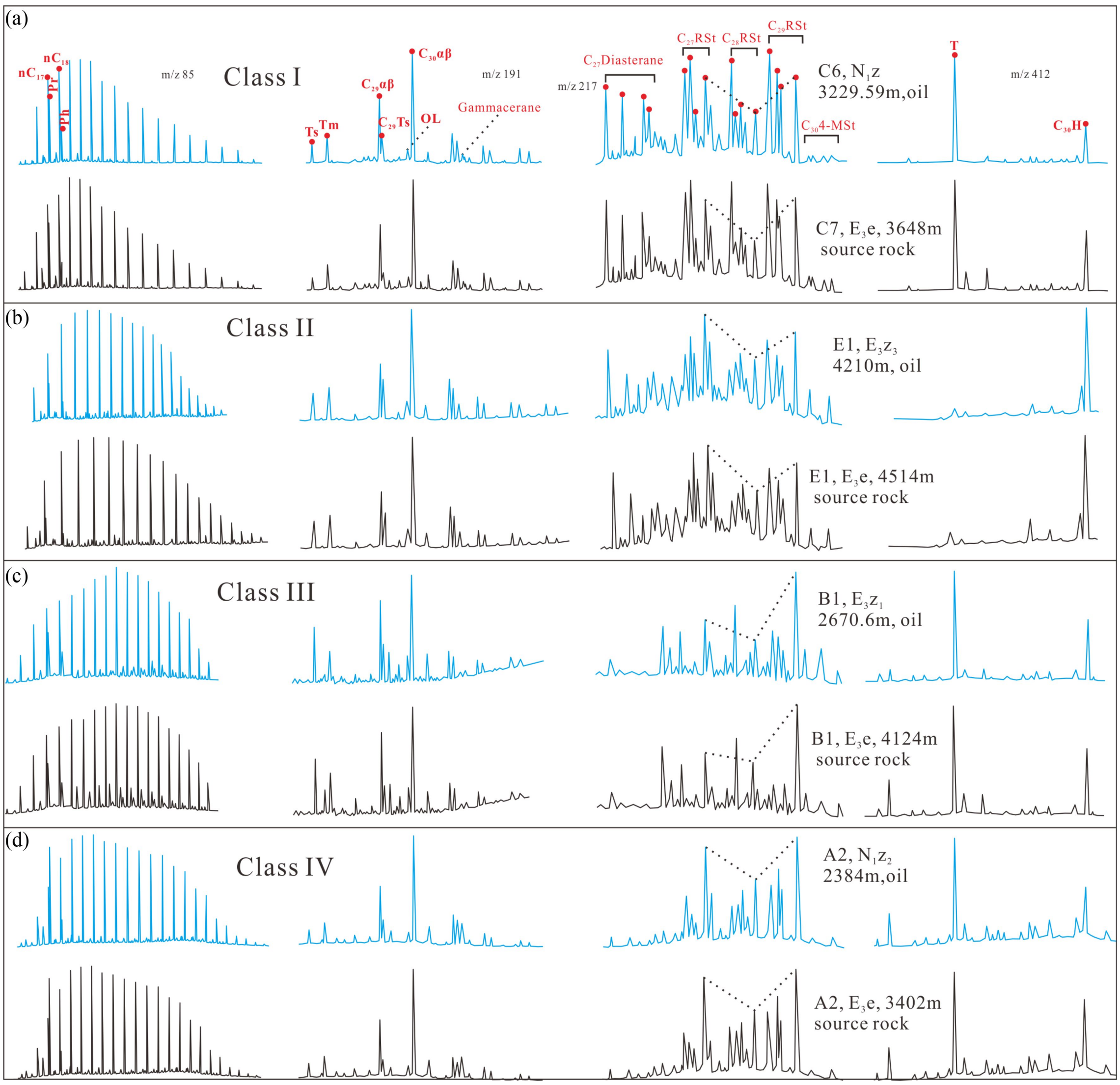

Fig. 7 TIC, m/z 191, m/z 217, and m/z 412 chromatograms of source rocks and crude oil from typical wells in the Wenchang-A Sag.

oil is distributed in Areas B and C, which is the crude oil of Wells B1 and C9.

The diasteranes content in class IV crude oil is low, and the regular steranes of $\alpha\alpha\alpha$20RC_{27}-$\alpha\alpha\alpha$20RC_{28}-$\alpha\alpha\alpha$20RC_{29} are distributed in 'V'-shaped distribution, with high peak bicadinane, (W + T)/C_{30}H value between 1.42 and 2.58, which is similar to the characteristics of source rocks in Area A. The crude oil of Wells A2 and C2 has these characteristics.

4.4 Geochemical characteristics of natural gas

4.4.1 Natural gas composition

Natural gas composition data are summarized in Table 4.

The chemical composition of natural gas in the study area changes significantly. A predominance of methane is observed in hydrocarbon gases. However, the methane content varies from 2.75% to 85.87%, with an average of 42.49%. The dryness coefficient (C_1/C_1 +) is 40.25%–90.19%, which indicates that natural gas is generally wet gas. Wells B5, D4, D5, and E1 are found with higher dryness coefficients (> 85%), while wells A2 and C4 are lower (< 60%). Variations in dryness coefficients may be related to organic matter types and maturity (Quan et al., 2019; Lu et al., 2021). In terms of non-hydrocarbon gases, besides the lower H_2 content (up to 0.01%), considerable variation is observed in O_2, N_2, and CO_2. Specifically, the O_2 is 0.00%–17.02%, averaging 2.91%; the N_2, 0.58%–75.72%, averaging 12.05%; the CO_2, 0.19%–90.82%, averaging 26.13%.

4.4.2 Stable carbon isotope ratios of natural gas

The carbon isotope ratio of natural gas is an important carrier of geological information in natural as (James, 1983; Tilley et al., 2011). $\delta^{13}C_1$ in the study area ranges from −46.15 ‰ to −37.50 ‰; $\delta^{13}C_2$, from −34.70 ‰ to −28.41 ‰; $\delta^{13}C_3$, from −31.48 ‰ to −24.99 ‰; $\delta^{13}C_4$, from −30.86 ‰ to −26.25 ‰ (Table 4). $\delta^{13}CO_2$ lies between −28.16 ‰ and −4.11 ‰ and averages −10.69 ‰ (Table 4). The carbon isotope ratios of *n*-alkanes in the natural gas grow with the increasing carbon number ($\delta^{13}C_1 < \delta^{13}C_2 < \delta^{13}C_3 < \delta^{13}C_4$), and yet the reversal distribution of the carbon isotopes of propane and butanes is observed in some formation intervals of wells C2, C7, D4, and D5 ($\delta^{13}C_1 < \delta^{13}C_2 < \delta^{13}C_3 > \delta^{13}C_4$) (Table 4). This may be because the produced natural gas is a mixture of gases from the same source rock yet with varied maturity or genes (Dai, 1990; Zumberge et al., 2012).

4.4.3 Light natural gas hydrocarbons

Natural gas light hydrocarbons are usually used to characterize maturity and origin (Huang et al., 2014; Feng et al., 2016). The number of C_5-C_7 alkanes (*n*-C_5-C_7) is 0.20%–0.69%, averaging 0.34; that of the iso-alkanes C_5-C_7 (iso-C_5-C_7), 0.21%–0.68%, with an average of 0.49%; that of cycloalkanes (cyc-C_5-C_7), 0.05%–0.42%, with an average of 0.18% (Table 5). The content of *n*-alkanes and iso-alkanes is relatively high, yet the cycloalkanes content is low. The content of heptanes and isoheptanes can be used as alkylating measurements of the alkylating of light hydrocarbons in sediments (Feng et al., 2016; Gong et al., 2018; Liu et al., 2018). The heptane content of natural gas in the study area varies from 10.96 to 28.57 (averaging 18.00), while the isoheptane content is 1.00–4.25 (with an average of 2.28) (Table 5). Extended variation ranges of the two parameters indicate differences in maturity and parent material sources.

5 Discussion

5.1 Sources of crude oil

Based on the vitrinite reflectance of kerogen (Table 1) and maturity biomarker parameters (Figs. 8(a) and 8(b)), it is concluded that the source rocks in Wenchang-A Sag are mature and have good hydrocarbon-generating potential (Xiao et al., 2020). Although the crude oil in the study area is all mature (Fig. 8(c)), the oil maturity still varies among different areas and wells in the same area (Fig. 8(d)). For example, the crude oil maturity of wells A2 and A3, C1 and C2 are differentiated. According to the theory of hydrocarbon generation evolution (Hunt, 1979; Huang et al., 1984), the wax content of oil increases with deepening maturation. Therefore, the discrepancy in the wax content for crude oil in Wenchang-A Sag is believed to be attributed to varying maturity.

The Enping Formation is the main source rock, but the source rocks of different wells of different blocks are wildly varied. Due to organic matter types, crude oil and natural gas characteristics also change. Cross plots of the parameters that can reveal the differences between crude oil and source rocks, such as $\sum C_{27}$RSt/$\sum C_{29}$RSt, $\sum C_{27}$DiaS/$\sum C_{27}$RSt, and (W + T)/C_{30}H are drawn (Fig. 9). Class I crude oil and Class IV crude oil have a single source. Class I is similar to the source rock distribution in Area C. The data distribution of Class IV crude oil is similar to that of source rock in Well A2, indicating that this type of crude oil comes from source rock in area A. Class II crude oil and Class III crude oil have mixed source characteristics. Class II crude oil is similar to source rocks in D and E areas. The type III crude oil is similar to the source rocks of wells A1 and B1, indicating that the crude oil comes from both the source rocks of Areas A and B.

5.2 Geneses and sources of natural gas

5.2.1 Thermal maturity

Natural gas heptane and isoheptane are important in

Table 4 Data table of natural gas composition and carbon isotope in Wenchang-A Sag

Type	Well	Depth/m	Formation	Molecular composition/%												$\delta^{13}C_{PDB}$/‰					Dryness coefficient / %
				H_2	O_2	N_2	CO_2	C_1	C_2	C_3	iC_4	nC_4	iC_5	nC_5	C_6+	C_1	C_2	C_3	nC_4	CO_2	
Group I	B5	2670.6	E_3z	0.00	1.43	5.26	4.58	62.88	14.32	6.10	1.74	1.85	0.83	0.46	0.55	−40.45	−30.08	−27.33	−27.27	−10.20	70.87
	B5	3056.7	E_3z	0.00	12.94	49.79	15.37	18.84	2.35	0.51	0.06	0.07	0.02	0.01	0.04	−41.73	−32.35	−28.22	–	−14.30	86.03
	B5	3370.7	E_3z	0.00	2.03	8.69	16.41	62.50	7.51	2.21	0.22	0.34	0.05	0.03	0.01	−43.67	−32.72	−30.01	−29.72	−9.55	85.77
	C6	3229.59	E_3z	0.01	1.54	5.96	6.95	70.74	9.36	3.55	0.81	0.68	0.23	0.11	0.07	−43.43	−31.58	−28.66	−28.51	−13.98	82.70
	D2	3798.5	E_3z	0.00	2.09	11.54	82.78	2.75	0.45	0.22	0.05	0.07	0.03	0.02	0.01	−42.76	−30.39	−28.66	−27.90	−4.23	76.33
	D2	3971	E_3z	0.02	0.35	3.92	32.40	42.62	7.83	7.64	1.78	2.26	0.64	0.49	0.09	−42.48	−29.57	−27.57	−26.53	−5.84	67.28
Group II	C3	3855	E_3z	0.00	0.72	2.78	4.79	69.82	14.18	4.62	0.87	0.93	0.45	0.24	0.60	−44.84	−32.84	−28.14	−27.79	−13.84	76.13
	C4	3638	E_3z	0.00	2.49	8.43	3.20	34.55	19.73	16.23	5.02	6.43	1.91	1.18	0.79	−45.49	−31.66	−29.62	−29.50	−12.69	40.25
	C7	3680.55	E_3e	0.00	0.51	2.07	67.41	22.98	4.47	1.44	0.33	0.33	0.17	0.10	0.20	−41.73	−31.14	−26.65	−26.46	−4.69	76.60
	C7	3799.9	E_3e	0.00	4.22	16.68	65.39	10.48	1.86	0.95	0.10	0.18	0.05	0.04	0.05	−43.64	−32.99	−30.68	−28.46	−4.58	76.41
	C7	3915.5	E_3e	0.00	1.72	6.71	68.86	18.43	3.04	0.79	0.14	0.14	0.06	0.03	0.07	−39.00	−30.21	−26.77	−27.10	−4.98	81.17
	C7	3954.5	E_3e	0.00	1.61	6.28	77.14	11.86	2.16	0.60	0.11	0.11	0.05	0.03	0.05	−39.88	−31.32	−26.60	−26.25	−5.07	79.21
	C7	3981	E_3e	0.00	0.52	2.22	87.14	7.57	1.48	0.50	0.12	0.13	0.09	0.06	0.18	−41.12	−29.90	−26.45	−26.54	−4.76	74.79
	D4	2871.5	E_3z	0.00	0.42	2.23	15.90	66.07	9.87	3.31	0.85	0.69	0.31	0.16	0.20	−40.66	−30.03	−27.86	−28.34	−9.43	81.11
	D4	3153	E_3z	0.03	16.62	70.37	1.33	10.27	0.96	0.28	0.06	0.05	0.02	0.01	0.01	−40.80	−30.96	−24.99	−27.94	−18.83	88.15
	D4	3306	E_3z	0.03	17.02	75.72	0.19	6.23	0.61	0.14	0.03	0.02	0.01	0.00	0.00	−43.77	−31.82	−28.19	–	−22.46	88.41
	D4	3391.6	E_3z	0.00	0.49	2.20	28.00	55.82	8.89	3.03	0.64	0.54	0.19	0.10	0.10	−42.90	−32.16	−29.04	−27.59	−7.22	80.53
	D4	3577	E_3z	0.00	0.28	1.23	28.21	53.56	10.17	3.76	0.84	0.87	0.46	0.26	0.39	−43.08	−32.41	−29.58	−29.14	−8.07	76.20
	D4	3670	E_3z	0.00	0.36	1.77	37.78	47.73	7.65	2.80	0.61	0.63	0.28	0.15	0.24	−43.25	−31.85	−28.48	−28.20	−9.22	79.44
	E2	3883.2	E_3e	0.00	0.44	2.30	4.23	71.73	12.68	6.91	0.85	0.64	0.13	0.05	0.03	−40.10	−32.05	−30.96	−29.58	−23.41	77.11

(*continued*)

Type	Well	Depth/m	Formation	Molecular composition/%												$\delta^{13}C_{PDB}$/‰					Dryness coefficient / %
				H_2	O_2	N_2	CO_2	C_1	C_2	C_3	iC_4	nC_4	iC_5	nC_5	C_6+	C_1	C_2	C_3	nC_4	CO_2	
Group III	A2	2345	N_1z	0.01	3.07	11.88	4.59	45.53	15.07	11.16	2.73	3.88	0.61	1.39	0.08	−41.87	−29.96	−26.88	−26.76	−9.12	56.59
	A2	2349	N_1z	0.00	1.82	8.09	3.67	39.31	17.61	15.60	4.23	6.00	1.09	2.43	0.15	−41.86	−29.57	−26.86	−26.70	−9.03	45.49
	A2	2350	E_3z	0.01	0.00	1.05	5.34	52.98	17.53	12.98	3.18	4.51	0.71	1.62	0.09	−45.01	−29.72	−26.70	–	−16.07	56.60
	A2	2352	E_3z	0.00	0.00	1.75	4.00	42.87	19.21	17.02	4.61	6.54	1.19	2.65	0.16	−45.01	−30.03	−26.66	–	−16.00	45.49
	A2	3276.5	N_1z	0.00	2.29	8.45	6.61	65.01	12.04	3.77	0.63	0.77	0.13	0.28	0.02	−37.99	−28.41	−26.97	−26.46	−12.43	78.66
	B6	2560.3	E_3z	0.00	10.67	45.06	33.30	9.09	1.07	0.42	0.09	0.11	0.05	0.03	0.11	−40.46	−30.95	−27.62	−27.51	−6.42	82.86
	B6	2904	E_3z	0.00	8.27	33.82	36.10	16.65	2.93	1.21	0.28	0.32	0.14	0.09	0.19	−42.07	−31.79	−28.54	−28.43	−5.21	76.34
	C2	3897	E_3z	0.00	0.84	3.31	8.29	64.77	13.60	5.38	1.16	1.34	0.58	0.32	0.41	−42.67	−32.39	−28.74	−28.17	−10.24	73.98
	C2	3900	E_3z	0.00	0.14	0.58	9.17	69.39	13.54	4.67	0.89	0.94	0.34	0.18	0.18	−42.77	−31.32	−27.92	−28.88	−9.42	77.00
	C2	3946	E_3z	0.00	1.48	6.35	12.25	49.34	15.32	10.93	1.55	1.98	0.43	0.23	0.13	−46.15	−34.70	−31.48	−30.86	−28.16	61.74
	D5	3349.5	N_1z	0.02	0.33	3.66	90.82	4.29	0.52	0.21	0.05	0.05	0.03	0.02	0.01	−41.55	−29.42	−27.76	−26.92	−4.86	82.95
	D5	3352	N_1z	0.00	1.48	8.73	85.88	3.28	0.39	0.14	0.03	0.04	0.01	0.01	0.00	−41.64	−29.24	−26.81	−26.84	−4.11	83.97
	D5	3400	E_3z	0.00	O.322	0.98	4.56	81.96	7.74	2.88	0.65	0.70	0.25	0.14	0.15	−38.14	−29.42	−28.27	−28.81	−12.09	86.76
	D5	3473	E_3z	0.00	5.21	19.87	2.41	63.85	5.77	1.70	0.41	0.36	0.17	0.09	0.17	−37.50	−29.11	−26.83	−28.10	−10.93	88.05
	D5	3523	E_3z	0.00	0.35	0.98	4.57	83.26	7.46	2.18	0.52	0.41	0.16	0.07	0.05	−38.49	−29.43	−26.99	−27.98	−11.95	88.47
	D5	3752.6	E_3z	0.00	0.55	2.90	5.20	47.36	17.60	14.17	3.72	3.79	1.62	1.06	2.04	−38.04	−28.92	−26.99	−26.99	−10.68	51.84
	E1	3714.1	E_3z	0.01	0.61	2.18	1.98	85.87	6.84	1.67	0.36	0.28	0.11	0.05	0.03	−37.58	−29.76	−29.12	−26.99	−11.33	90.19

Note: "–" no data.

Table 5 Data table of natural gas light hydrocarbon in Wenchang-A Sag

Type	Well	Depth/m	Formation	Cyc-C_5-C_7/%	n-C_5-C_7/%	Iso-C_5-C_7/%	Heptane/%	Iso-heptan/%	Type	Well	Depth/m	Formation	Cyc-C_5-C_7/%	n-C_5-C_7/%	Iso-C_5-C_7/%	Heptane/%	Iso-heptan/%
Group I	B5	2968	E_3z	0.11	0.58	0.31	19.88	1.57	Group II	D4	2871.5	E_3z	0.09	0.25	0.66	18.00	4.25
	C5	3230	E_3z	0.10	0.45	0.45	18.18	3.00		D4	3391.6	E_3z	0.09	0.27	0.65	18.60	3.25
	C5	3390	E_3z	0.16	0.35	0.49	15.79	2.75		D4	3393.5	E_3z	0.18	0.25	0.58	19.79	2.86
	C5	3490	E_3z	0.21	0.37	0.42	17.72	2.42		D4	3577	E_3z	0.12	0.26	0.62	20.00	2.10
	C5	3502	E_3z	0.15	0.40	0.45	17.60	2.56		D4	3670	E_3z	0.11	0.26	0.63	16.42	2.86
	C6	3213	E_3z	0.22	0.34	0.44	15.79	3.67	Group III	E2	3883.2	E_3e	0.25	0.25	0.51	10.96	1.00
	C6	3215	E_3z	0.19	0.41	0.40	16.13	2.25		A2	2350	N_1z	0.08	0.34	0.58	16.47	3.75
	C6	3229.59	E_3z	0.07	0.39	0.54	18.18	2.00		A2	3276.5	N_1z	0.16	0.30	0.55	13.89	2.50
	D2	3349.5	E_3z	0.10	0.69	0.21	20.00	1.50		B6	2405	E_3z	0.24	0.33	0.43	17.09	1.56
	D2	3352	E_3z	0.10	0.69	0.21	20.00	1.50		B6	2407	E_3z	0.22	0.34	0.44	16.67	1.84
	D2	3798.5	E_3z	0.22	0.47	0.31	21.12	1.09		B6	2411	E_3z	0.22	0.34	0.45	16.79	2.21
	D2	3814	E_3z	0.18	0.57	0.26	13.33	1.00		B6	2465	E_3z	0.22	0.34	0.44	15.06	1.82
	D2	3971	E_3z	0.12	0.66	0.22	26.84	1.52		B6	2468	E_3z	0.21	0.37	0.42	14.75	1.93
Group II	C3	3425	E_3z	0.17	0.28	0.55	19.65	1.28		B6	2491	E_3z	0.18	0.38	0.44	17.17	2.08
	C3	4051	E_3z	0.25	0.30	0.45	16.05	1.56		B6	2492	E_3z	0.20	0.36	0.44	16.22	1.93
	C3	4102.7	E_3z	0.27	0.28	0.46	16.47	1.13		B6	2507	E_3z	0.23	0.35	0.42	16.85	2.05
	C3	4145	E_3z	0.28	0.26	0.46	12.32	1.82		B6	2525	E_3z	0.22	0.35	0.43	14.94	2.22
	C4	3638	E_3z	0.05	0.29	0.66	20.59	3.00		B6	2540	E_3z	0.20	0.35	0.46	17.09	2.38
	C4	3995	E_3z	0.15	0.24	0.61	11.76	1.22		B6	2560.3	E_3z	0.22	0.31	0.47	14.81	1.77
	C4	4067	E_3z	0.16	0.24	0.60	12.09	1.27		B6	2563	E_3z	0.17	0.34	0.49	13.33	2.20
	C7	3799.9	E_3e	0.17	0.29	0.54	20.39	2.45		B6	2580	E_3z	0.23	0.34	0.43	17.70	2.36
	C7	3860.55	E_3e	0.15	0.21	0.64	20.00	3.00		B6	2902	E_3z	0.21	0.32	0.47	14.06	2.00
	C7	3865.55	E_3e	0.08	0.24	0.68	18.00	3.40		B6	2904	E_3z	0.25	0.35	0.40	18.64	2.06
	C7	3915.5	E_3e	0.14	0.22	0.64	20.24	3.13		D5	3287	N_1z	0.27	0.30	0.43	21.52	3.29
	C7	3954.5	E_3e	0.13	0.22	0.64	20.48	3.13		D5	3473	N_1z	0.42	0.26	0.32	25.82	2.66
	C7	3981	E_3e	0.16	0.20	0.64	19.17	3.21		D5	3752.6	N_1z	0.38	0.25	0.38	25.57	2.42
	C8	3521	E_3z	0.20	0.30	0.50	18.31	2.63		E1	3695	E_3z	0.11	0.34	0.56	21.43	1.00
	C8	3648	E_3z	0.16	0.26	0.59	26.36	2.18		E1	3714.1	E_3z	0.08	0.25	0.67	16.13	3.67
	C8	3692	E_3z	0.17	0.27	0.56	16.36	2.83		E1	4162	E_3z	0.15	0.31	0.53	18.47	2.31

Notes: n-C_5-C_7: normal C_5-C_7 alkanes; iso-C_5-C_7: iso-alkanes C_5-C_7; cyc-C_5-C_7: cycloalkanes C_5-C_7. Heptane (%) = n-C_7 × 100/ (CH + 2 MH + 2,3DMP + 1,1DMCP + 3 MH + c1,3DMCP + t1,3DMCP + t1,2DMCP + 3 EP + 2,2,4TMP + n-C_7 + MCH); Iso-heptane (%) = (2 MH + 3 MH) × 100/(t1,2DMCP + c1,3DMCP + t1,3DMCP) (Huang et al., 2014).

determining maturity and organic matter types. Thompson (1983) proposes two empirical curves for determining parent material types, and Cheng et al. (1987) develop criteria for determining maturity. Group I natural gas is between aliphatic and aromatic, mature natural gas. Group II is close to the aromatic line, most of which are mature natural gas, and some of which are highly mature. Group III has the characteristics of the first two gas groups (Fig. 10(a)).

Carbon isotope ratios among different components of natural gas change significantly with maturity, which is commonly used for maturity identification (James, 1983). Our calculation shows (Fig. 10(b)) the carbon isotope ratio is consistent with the theoretical line (James, 1983; Wang et al., 2022), yet with scattered distribution (mainly of 0.7%–1.2%). Accordingly, natural gas is attributed to the mature stage. Group III gas data are widely distributed and vary widely in maturity. The inverse distribution of carbon isotope ratios of propane and butanes in group III (Table 4) can be attributed to the mixing of natural gas with varying maturity in these gasses.

5.2.2 Sources of natural gas

The origins of natural gas can be identified according to

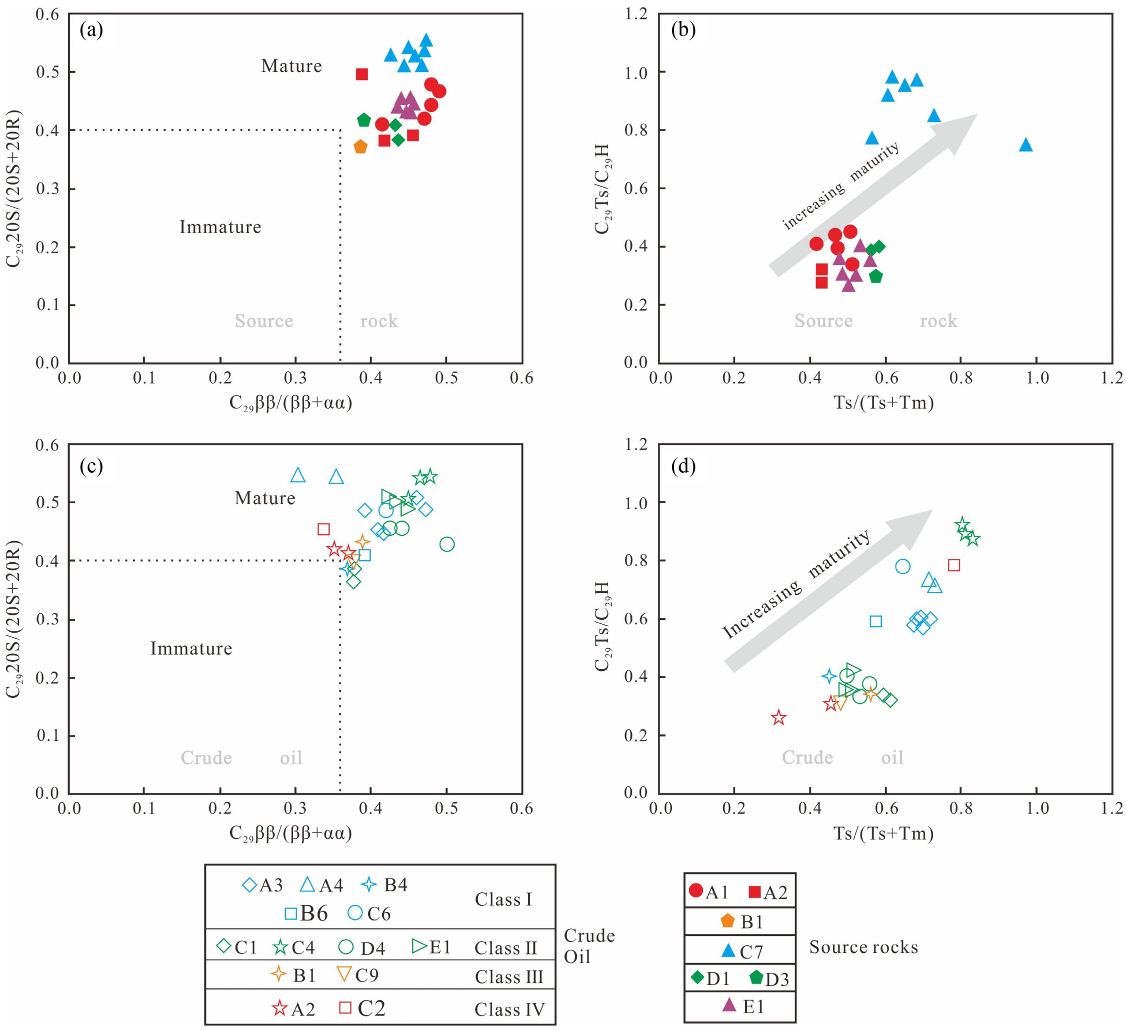

Fig. 8 The scatter plots of maturity biomarkers for source rocks (a, b) and those for crude oil (c, d) in Wenchang-A Sag.

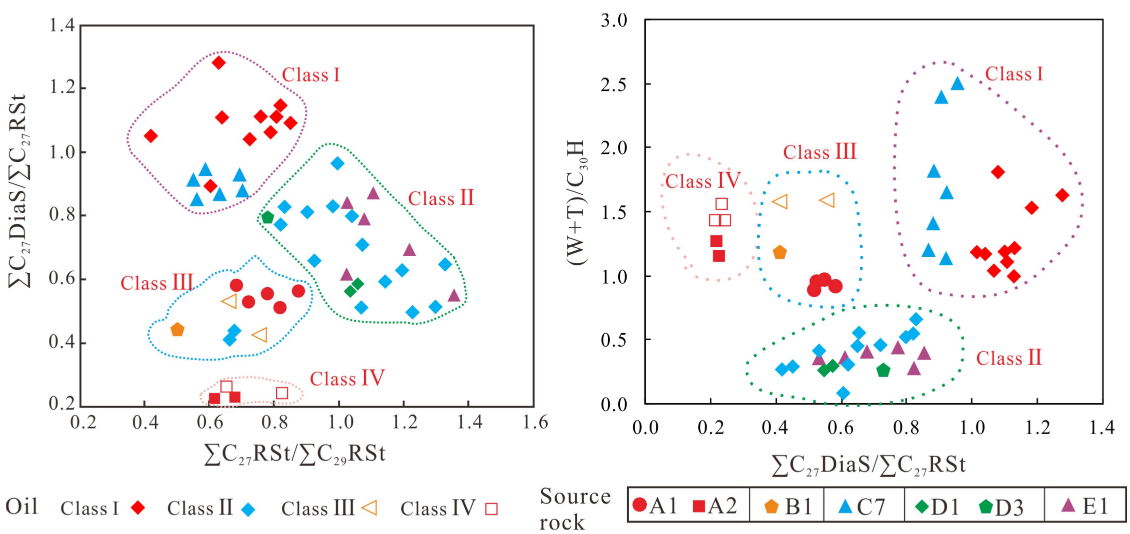

Fig. 9 Biomarker scatterplots of regular steranes and bicadinanes from crude oil and source rocks in Wenchang-A Sag.

the measurements of natural gas composition and carbon isotope ratios (Wood and Hazra, 2017; Milkov, 2018). The organic and inorganic gases can be distinguished using the carbon isotope ratios of natural gas components. With the increasing carbon number, the carbon isotope ratios of biogenetic gas grow, while the case of inorganic gas is just the opposite (Chung et al., 1988; Dai, 1990; Tilley et al., 2011). The natural gas features $\delta^{13}C_1$ <

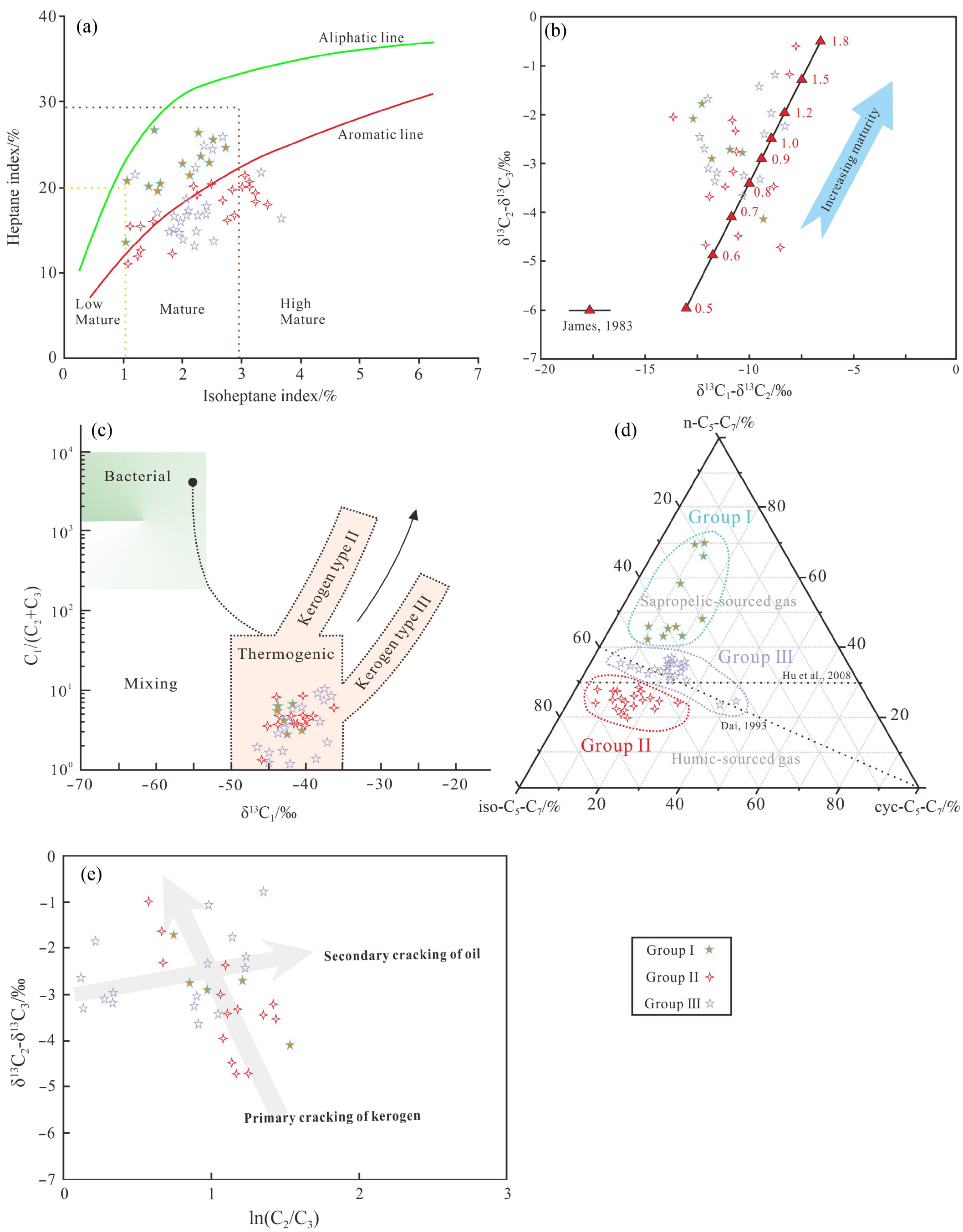

Fig. 10 (a) The scatter plot of heptane and isoheptane values of natural gas light hydrocarbons in Wenchang-A Sag (modified from Quan et al. (2019), and calculation formulas for heptane and isoheptane values from Huang et al. (2014)). (b) Scatter diagram of maturity determination by carbon isotope difference of alkane gas in Wenchang-A Sag (The theoretical curve was established by James (1983)). (c) Relationship diagram of natural gas $\delta^{13}C_1$ and $C_1/(C_2 + C_3)$ in Wenchang-A Sag (modified from Whiticar, 1999). (d) Triangular diagram of natural gas C_5-C_7 light hydrocarbons in Wenchang-A Sag (Baseline reference from Hu et al., 2008). (e) The relationship diagram of $\delta^{13}C_2 - \delta^{13}C_3$ and ln (C_2/C_3) of natural gas in Wenchang-A Sag (modified from Prinzhofer and Huc, 1995).

$\delta^{13}C_2 < \delta^{13}C_3 < \delta^{13}C_4$, with the distribution reversal found between propanes and butanes of some samples (Table 4). For hydrocarbon gases, the methane carbon isotope ratio of the biogenetic gas is typically below −30 ‰ (Whiticar, 1999). To sum up, the hydrocarbon gases of the Wenchang-A Sag are identified as biogenetic gas. And it’s all thermogenic gas (Fig. 10(c)).

The light hydrocarbon content depends on the types of organic matter. Specifically, gas from sapropelic organic matter has a relatively higher content of *n*-alkanes, while that originating from humic organic matter has a higher content of iso-alkanes and cycloalkanes (Leythaeuser et al., 1979). Group I of natural gas comes from sapropelic parent material, Group II is humic parent

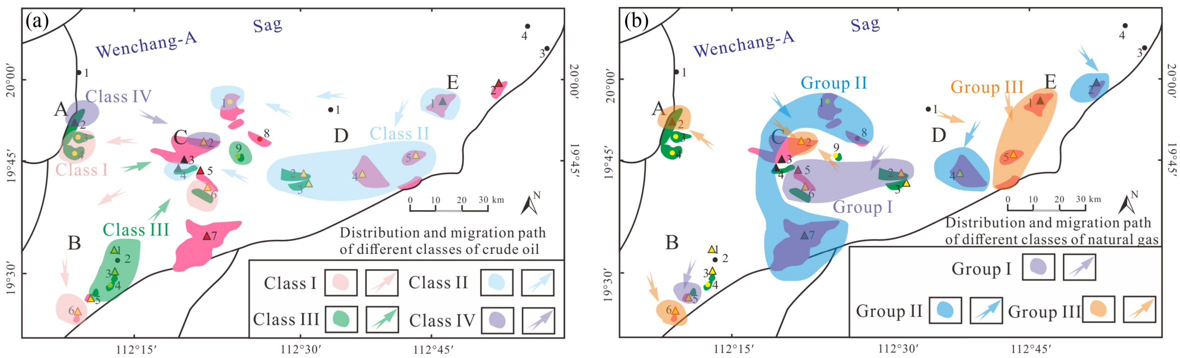

Fig. 11 (a) The distribution and source of four classes of crude oil, (b) The distribution and source of three groups of natural gas.

material. Group III is distributed near the boundary, with mixed source characteristics (Fig. 10(d)). Comparison with the planar distribution of organic matter types of the source rocks (Fig. 3) shows that the parent material types of natural gas are consistent with the organic matter types of the source rocks. In other words, the differentiation of natural gas types across the study area is mainly caused by the variation of organic matter types.

According to hydrocarbon generation theory (Hunt, 1979; Huang et al., 1984), humus-like organic matter can generate natural gas through kerogen cracking during the mature stage, and crude oil can also produce natural gas via cracking. To identify cracking types of natural gas in the Wenchang-A Sag, the chart proposed by Prinzhofer and Huc (1995) is adopted (Fig. 10(e)). Groups I and II have negative slope change characteristics, i.e., kerogen cracking gas. However, Grope III has horizontal variation characteristics but also longitudinal variation characteristics, mainly crude oil secondary cracking gas and also kerogen cracking gas characteristics.

5.3 Exploration significance

The distribution of oil and gas reservoirs in the Wenchang-A sag is complex due to multiple small sub-sags. Class I crude oil is sporadically distributed in Areas A, B, and C, and comes from source rocks in Area C (Fig. 11(a)). Class II crude oil is widely distributed in Area D and less in E and C areas. Crude oil comes from source rocks in Areas D and E (Fig. 11(a)). Class III crude oil is mainly distributed in Area B and there is a small amount in Area C. The oil source is the source rocks in Areas A and B. Class IV crude oil distribution area is small, only in Areas A and C, which comes from source rocks in Area A (Fig. 11(a)). In summary, the crude oil in the study area is mainly derived from local source rocks. Source rocks in adjacent sub-sags also contribute. In the future, exploration can continue in Areas C and D to find reservoirs.

Natural gas in Groups I and II is derived from local source rocks, and the natural gas in Group III has mixed source characteristics (Fig. 11(b)). The type of natural gas is closely related to the type of source rock organic matter. Future gas reservoirs are concentrated in Areas C, D, and E.

6 Conclusions

1) The Enping Formation source rocks of the Wenchang-A Sag have significant differences in different areas. The source rocks throughout the sag have entered the mature stage, with R_o of 0.70%−1.29%. The hydrocarbon generation potential of source rocks in the central sag is higher than that in the sag margin. In terms of organic matter types, the planar distribution shows that Areas A, B, and D have more sapphire-type source rocks, while Areas C and E are found with more humic-type rocks.

2) The reservoirs of Wenchang-A Sag are concentrated in the development zone of the more-sapropelic source rocks and have low-density light oil. The wax content of oil varies greatly due to products of different maturation stages. According to the physical properties and biomarker parameters, crude oil is divided into four classes. Classes I and IV crude oil come from local source rocks. Classes II and III have mixed source characteristics. Class II comes from source rocks in Areas D and E, and class III comes from Areas A and B.

3) The natural gas in the study area is mostly mature. Mixing natural gas with varying maturity results in the reversal distribution of carbon isotope ratios of hydrocarbon gases, which are mainly thermogenic. Group I is sapropelic gas, Group II is humic gas, and Group III has mixed source characteristics. Groups I and II gas are kerogen cracking gas, group III has both crude oil secondary cracking gas and kerogen cracking gas characteristics. The parent material types of natural gas are consistent with the planar distribution of organic matter types of source rocks.

Acknowledgment Funding for this research came from the Southwest Petroleum University 2021 Graduate Research and Innovation Fund (No. 2021CXYB27), the National Natural Science Foundation of China (Grant Nos. 41872165 and 42072185), and the development mechanism of high-quality source rocks and hydrocarbon accumulation regularity in the Zhusan Depression (No. CCL2020ZJFN0226).

Competing interest: The authors declare that they have no competing interests.

References

Chen L, Fan C W, Liu X Y, Li M, Lei M Z (2021). Hydrocatbon enrichment laws and favourable exploration directions of Wenchang A sag, western Pearl River Mouth Basin. China Offshore Oil and Gas, 33(5): 14–23 (in Chinese)

Chen Y, Mi T Z, Liu Y T, Li S Q, Zhen Y (2020). Microbial community composition and function in sediments from the Pearl River Mouth Basin. J Ocean Univ China, 19(4): 941–953

Cheng K, Jin W, He Z, Chen J, Yang Z (1987). Composition characteristics of light hydrocarbons in continental oil and condensate and their geological significance. Petrol Explor Dev, 1: 34–43+33 (in Chinese)

Cheng P, Xiao X M, Gai H F, Li T F, Zhang Y Z, Huang B J, Wilkins R W T (2015). Characteristics and origin of carbon isotopes of *n*-alkanes in crude oils from the western Pearl River Mouth Basin, South China Sea. Mar Pet Geol, 67: 217–229

Chung H M, Gormly J R, Squires R M (1988). Origin of gaseous hydrocarbons in subsurface environments: theoretical considerations of carbon isotope distribution. Chem Geol, 71(1−3): 97–104

Dai J (1990). A brief discussion on the problem of the geneses of the carbon isotopic series reversal in organogenic alkane gases. Nat Gas Ind, 10(6): 15–20 (in Chinese)

Dehyadegari E (2021). Geochemistry and origins of Sarvak oils in Abadan plain: oil-oil correlation and migration studies. Energy Sources A Recovery Util Environ Effects, 43(6): 716–726

Feng Z, Liu D, Huang S, Gong D, Peng W (2016). Geochemical characteristics and genesis of natural gas in the Yan'an gas field, Ordos Basin, China. Org Geochem, 102: 67–76

Fu N, Li Y C, Sun X, Sun Y M, Xu J Y (2011). Recognition of oil source and source rocks in Zhu III Depression. Geoscience, 25(06): 1121–1130 (in Chinese)

Gong D, Li J, Ablimit I, He W, Lu S, Liu D, Fang C (2018). Geochemical characteristics of natural gases related to Late Paleozoic coal measures in China. Mar Petrol Geol, 96: 474–500

Hu G, Li J, Li J, Li Z, Luo X, Sun Q, Ma C (2008). Preliminary study on the origin identification of natural gas by the parameters of light hydrocarbon. Sci China Ser D Earth Sci, 51(S1): 131–139

Huang B J, Xiao X M, Zhang M Q (2003). Geochemistry, grouping and origins of crude oils in the Western Pearl River Mouth Basin, offshore South China Sea. Org Geochem, 34(7): 993–1008

Huang D F, Li J C, Zhou N H, Gu X Z, Zhang D J (1984). The evolution of continental organic matter and the mechanism of hydrocarbon generation. Beijing: Petroleum Industry Press (in Chinese)

Huang D F, Zhang D J, Li J C (1994). The origin of 4-methyl steranes and pregnanes from Tertiary strata in the Qaidam Basin, China. Org Geochem, 22(2): 343–348

Huang S, Wang Z, Lv Z, Gong D, Yu C, Wu W (2014). Geochemical identification of marine and terrigenous condensates—a case study from the Sichuan Basin, SW China. Org Geochem, 74: 44–58

Huang W B, Cheng J, Shao M L (2022). Discussion on organic matter abundance evaluation criteria of source rocks in deep middle-high thermal evolution stage in south Songliao Basin. Unconventional Oil & Gas, 8(2): 13–23 (in Chinese)

Hunt J (1979). Petroleum Geochemistry and Geology. San Francisco: Freeman W. H.

James A T (1983). Correlation of natural gas by use of carbon isotopic distribution between hydrocarbon components. AAPG Bull, 67(7): 1176–1191

Jiang H, Wang H, Li J L, Chen S P, Lin Z L, Fang X X, Cai J (2009). Research on hydrocarbon pooling and distribution patterns in the Zhu-3 Depression, the Pearl River Mouth Basin. Oil Gas Geol, 30: 275–281+286 (in Chinese)

Jiang W M, Li Y, Yang C, Xiong Y Q (2021). Organic geochemistry of source rocks in the Baiyun Sag of the Pearl River Mouth Basin, South China Sea. Marine and Petroleum Geology, 124: 104836

Leythaeuser D, Schaefer R G, Cornford C, Weiner B (1979). Generation and migration of light hydrocarbons (C_2-C_7) in sedimentary basins. Org Geochem, 1(4): 191–204

Li X Y, Gong Y (2022). Differences in organic matter between coal and gangue of Shanxi Formation and Taiyuan Formation in Yanchuannan. Unconventional Oil Gas, 9(6): 27–27 (in Chinese)

Li Y, Chen S J, Wang Y X, Qiu W, Su K M, He Q B, Xiao Z L (2019). The origin and source of the Devonian natural gas in the Northwestern Sichuan Basin, SW China. J Petroleum Sci Eng, 181: 106259

Liu Y, Chen D, Qiu N, Fu J, Jia J (2018). Geochemistry and origin of continental natural gas in the western Sichuan Basin, China. J Nat Gas Sci Eng, 49: 123–131

Lu J G, Luo Z Y, Zou H L, Li Y P, Hu Z Z, Zhou Z Y, Zhu J, Han M M, Zhao L P, Lin, Z H (2021). Geochemical characteristics, origin, and mechanism of differential accumulation of natural gas in the carboniferous kelameili gas field in Junggar Basin, China. J Petroleum Sci Engineering, 203: 108658

Lu K N (2021). Study on classification and evaluation of deep source rocks and their accumulation relations in Dehui Fault Depression. Unconventional Oil Gas, (06): 14–23 (in Chinese)

Milkov A V (2018). Secondary microbial gas. In: Wilkes H, ed. Hydrocarbons, Oils and Lipids: Diversity, Origin, Chemistry and Fate. Handbook of Hydrocarbon and Lipid Microbiology. Cham: Springer

Peters K, Cassa M (1994). Applied source rock geochemistry. In: Magoon L, Dow W, eds. AAPG Memoir 60, the Petroleum System - from Source to Trap. AAPG, Tulsa: 93–120

Prinzhofer A A, Huc A Y (1995). Genetic and post-genetic molecular and isotopic fractionations in natural gases. Chem Geol, 126(3−4): 281–290

Quan Y B (2018). Lacustrine source rock development mechanism and its contribution to hydrocarbon accumulation in Zhu III sub-basin, Pearl River Mouth Basin. Dissertation for Doctoral Degree. Wuhan: China University of Geosciences (in Chinese)

Quan Y B, Liu J Z, Hao F, Bao X H, Xu S, Teng C Y, Wang Z F (2019). Geochemical characteristics and origins of natural gas in the Zhu III subbasin, Pearl River Mouth Basin, China. Mar Pet Geol, 101: 117–131

Quan Y B, Liu J Z, Zhao D J, Hao F, Wang Z F, Tian J Q (2015). The origin and distribution of crude oil in Zhu III sub-basin, Pearl River Mouth Basin, China. Mar Pet Geol, 66(4): 732–747

Su K M, Chen S J, Hou Y T, Zhang H F, Zhang X L, Zhang W X, Liu G L, Hu C, Han M M (2021). Geochemical characteristics, origin of the Chang 8 oil and natural gas in the south western Ordos Basin, China. J Petroleum Sci Eng, 200: 108406

Tang L X, Zhou H, Yin L L (2022). Analysis on organic geochemistry characteristics and hydrocarbon-generating potential of coal-bearing strata in Huaibei Area. Unconventional Oil Gas, 9(6): 51–60,74 (in Chinese)

Thompson K F M (1983). Classification and thermal history of petroleum based on light hydrocarbons. Geochimica et Cosmochimica Acta, 47(2): 303–316

Tilley B, Mclellan S, Hiebert S, Quartero B, Veilleux B, Muehlenbachs K (2011). Gas isotope reversals in fractured gas reservoirs of the western Canadian Foothills: mature shale gases in disguise. AAPG Bull, 95(8): 1399–1422

Tissot B P, Welte D G (1984). Petroleum Formation and Occurrence, second ed. Berlin: Springer-Verlag, 699

Wang X Z, Cao H X, Cao J (2022). Analysis of natural gas source of Lower Paleozoic in Yan'an Area, Ordos Basin. Unconventional Oil Gas, 9(6): 9–13 (in Chinese)

Whiticar M (1999). Carbon and hydrogen isotope systematics of bacterial formation and oxidation of methane. Chem Geol, 161(1−3): 291–314

Wood D A, Hazra B J (2017). Characterization of organic-rich shales for petroleum exploration & exploitation: a review-Part 2: geochemistry, thermal maturity, isotopes and biomarkers. J Earth Sci, 28(5): 758–778

Wu C L (1984). Nan Hai (the South China Sea) movement and development of basins in the South China Sea. Mar Sci Bull, 3: 47–53 (in Chinese)

Wu L Y, Gu X Z (1986). The application of pyrolysis technique in source rocks research. Acta Petrol Sin, 7(2): 13–19

Xiao X M, Li N H, Gan H J, Tian H, Huang B J, Tang Y C (2009). Tracing of deeply-buried source rock: a case study of the WC9–2 petroleum pool in the Pear River Mouth Basin, South China Sea. Marine Petroleum Geo, 26: 1365–1378

Xiao Z L, Chen S J, Li Y, Su K M, He Q B, Han M M (2020). Local high-salinity source rock and origin of crude oil in the Xianshuiquan Structure in the northwestern Qaidam Basin, China. J Petrol Sci Eng, 198: 108233

Xu X D, Huang B J (2000). A Study on the migration and accumulation of oil and gas in Qionghai ulift, Zhusan depression. Petroleum Explor Develop, 27 (4): 41–44+111–120 (in Chinese)

Zumberge J, Ferworn K, Brown S (2012). Isotopic reversal ('rollover') in shale gases produced from the Mississippian Barnett and Fayetteville formations. Mar Petrol Geol, 31(1): 43–52